Reply to comments

This manuscript describes a method for detecting water subduction associated with mesoscale eddies in the western North Pacific and estimates of the amount of material transported into the mesopelagic zone. The authors detected episodic subduction patches using spicity and oxygen anomalies from the BGC-Argo dataset. They found 288 subduction patches, most of which were observed between March and August in the Kuroshio Extension region. Most of subduction patches were found below the annual permanent thermocline depth (450 db). They estimated export rates of oxygen and carbon on the order of 175 to 417 mg O2 m-2 day-1 and 85 to 159 mg C m-2 day-1. The method used in this manuscript to detect subduction is very interesting. It is also an important finding that many subduction patches exist in the Kuroshio Extension region and that many of them are deeper than the permanent thermocline. On the other hand, it is important to know the distribution and amount of material transport by subduction, but the analysis and discussion are not sufficient. There are some problems with estimation the amount of material transported by subduction. I cannot recommend this manuscript for publication. I request significant revision and additional discussion.

Reply: Thanks for the critical and constructive comments to help us improve the manuscript. We carefully considered all the comments and addressed most of them in the revision, please see our detailed replies below.

Major comments

1) In this study, subduction patches were detected using a unique method. The spatial (horizontal and vertical) distributions of patches and seasonal variation of number of patches are discussed respectively, but it will be necessary to combine them. If the authors are going to discuss oxygen export by subduction, the patches must be considered separately shallower and deeper layers than the permanent pycnocline. Since the depth of permanent pycnocline differs between the subtropical and subarctic region, it is also necessary to distinguish between the regions.

Reply: This is a good point. In the revision, we examined how the subduction patches distributed over the study domain in each season, with results shown in Fig. 5c. In general, there were no spatial patterns of the subduction patches in each season. We clarified this in the main text.

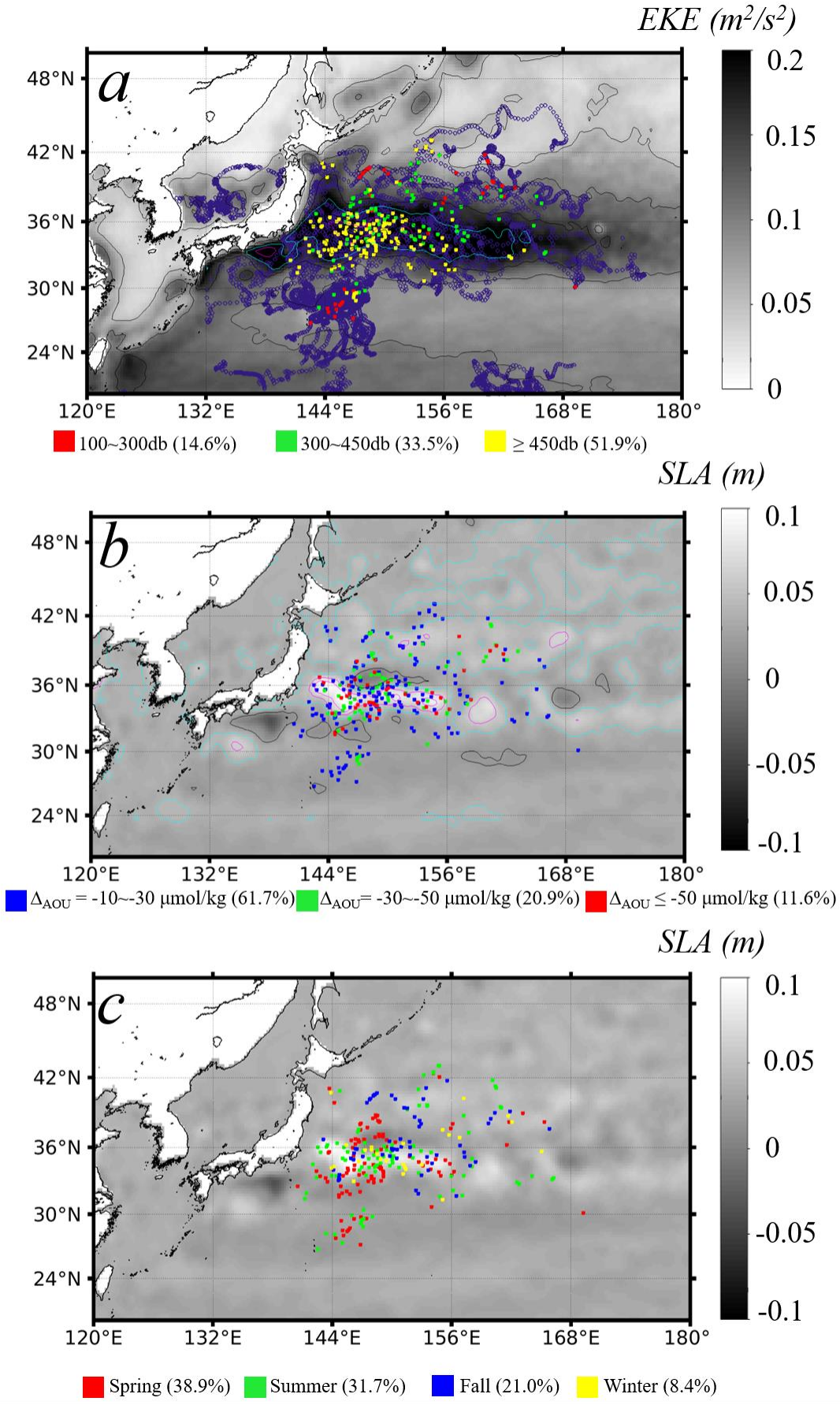
EKE (m²/s²)
a
48°N
42°N
36°N
30°N
24°N
120°E
132°E
144°E
156°E
168°E
180°
0.2
0.15
0.1
0.05
0
100~300db (14.6%)
300~450db (33.5%)
≥ 450db (51.9%)
SLA (m)
b
0.1
0.05
0
-0.05
-0.1
ΔAOU = -10~-30 µmol/kg (61.7%)
ΔAOU= -30~-50 µmol/kg (20.9%)
ΔAOU ≤ -50 µmol/kg (11.6%)
SLA (m)
c
0.1
0.05
0
-0.05
-0.1
Spring (38.9%)
Summer (31.7%)
Fall (21.0%)
Winter (8.4%)

Fig. 5 (updated). Horizontal distribution of the BGC-Argo data profiles associated with subduction patches (a and b) between 2008 and 2019 in the western North Pacific. The profiles with detected subduction patches are color coded by different intervals of depths of the subduction patches (a), AOU anomalies (b), and seasons (c), with percentages of detected patches in each interval annotated. The purple background data in (a) represent all the analyzed profiles as shown in Fig. 2a. The grey-scale background map in (a) is the annual mean EKE climatology, with EKE contour lines of 0.3, 0.2, and 0.1 m^2/s^2 shown in magenta, cyan, and black, respectively, and the grey-scale background map in (b) is the annual mean SLA climatology, with SLA contour lines of ≥ 0.06, 0.04, and 0.02 m shown in magenta, cyan, and black, respectively. The seasons in (c) is divided with Spring of March-May, Summer of June-August, Fall of September-November, and Winter of December-February.

Yes, one important factor about the sequestration time scales of the subduction patches is that whether these injections extend below the depth of permanent pycnocline (PP), which hinders their return to the atmosphere. The subduction patches above the depth of PP cannot be isolated for a long time because they would dissipate in the next year. The depth of PP differs between the subtropical section (i.e., south of 35° N) and subpolar section (i.e., north of 35° N) of the western North Pacific. Therefore, it is better to quantify the subduction patches separately for each section and for each depth (i.e., above or below the depth of PP).

Based on 16 years' Argo float data (which provides temperature and salinity profiles) (N=1,226,177), Feucher et al. (2019) investigated the distribution of the depth of permanent pycnocline in the world ocean. As outlined in the red box in Fig. R1, the depth of PP was shallower (≤300 m) and deeper (≥400-450m) depth of PP in the subpolar and subtropical sections of the western North Pacific, respectively. In addition, based on the 7120 profiles from the BGC-Argo floats (Fig. 2), we also analyzed the monthly dynamics of the maximum MLD with variance in both of the subtropical (i.e., south of 35° N) and subpolar (i.e., north of 35° N) sections of the western North Pacific. We took the annual maximum MLD as the potential depth of PP. It is seen that, in February and March, the maximum MLD was the deepest over the year in both sections, and values are comparable with those shown in Fig. R1 in Feucher et al. (2019), and more importantly, consistent with the spatial patterns shown in Fig. R1, our data also show that the annual maximum MLD (i.e., potential depth of PP) is shallower in the subpolar section, and deeper in the subtropical section. Mathematically, our data show that the annual maximum MLD with one standard deviation could reach 400 m, which is smaller than the maximum depth contours of PP (i.e., 450 m) identified in Feucher et al. (2019). However, it should be noted that, our result in Fig. R2 is quite preliminary based on a much smaller dataset than that in Feucher et al. (2019). With the analyses above, and to be conservative, we finally chose to use the maximum potential of PP depth of 300 m and 450m for the subpolar and subtropical sections, respectively, in our analysis of the subduction patches in each layer (i.e., above or below the depth of PP).

As a result, in the subtropical section (PP depth at 450 m), 104 (31.0%) and 56 (16.7%) subduction patches were found to below the depth the permanent pycnocline (i.e., 450

m); and in the subpolar section, 141 (42.1%) and 34 (10.1%) subduction patches were above the permanent pycnocline. This result was added in the revised manuscript.

In addition, we also separately quantified the average AOU and DO anomalies and DO inventories below and above the depth of permanent pycnocline for each section. Please see our replies to the following comment below.

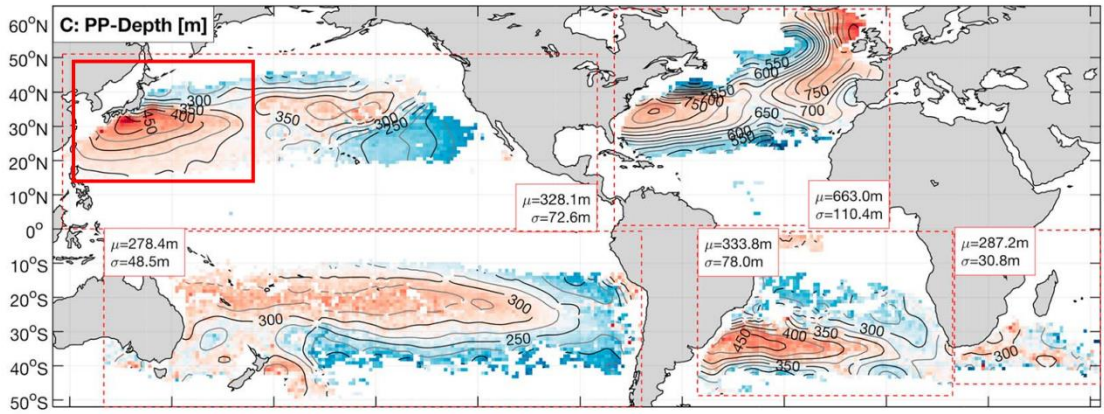

Fig. R1 The 2000-2015 Argo climatology of permanent pycnocline (PP) depth in the global ocean. Contours are every 25 m, labeled every 50 m. Cited from Fig. 2 in Feucher et al. (2019). Our study region is outlined in red.

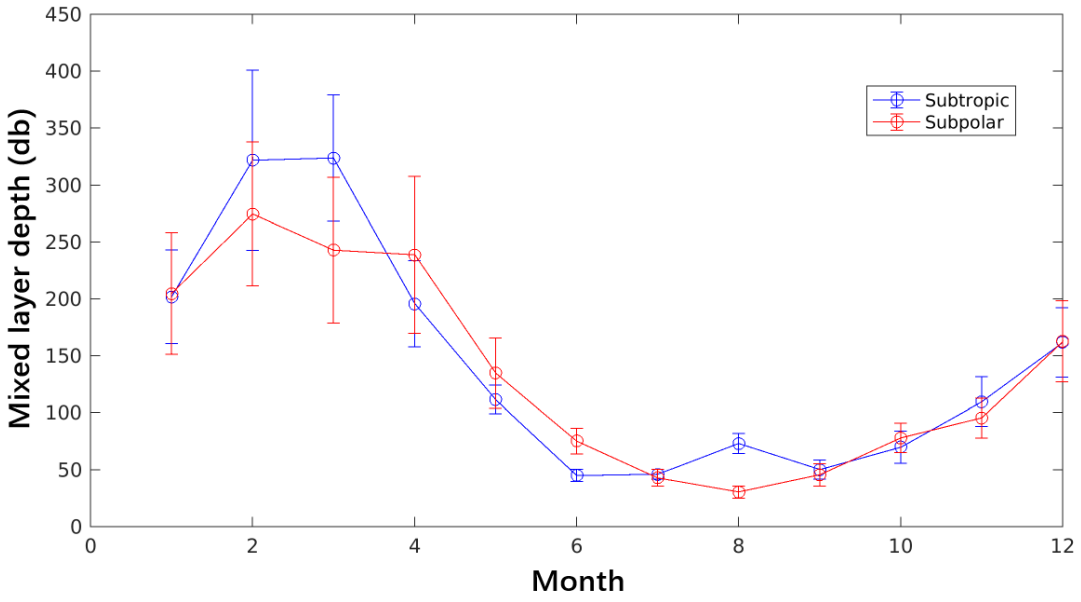

Fig. R2 The monthly variations of the maximum mixed layer depth (MLD) in the subtropical (i.e., south of 35° N) and subpolar (i.e., north of 35° N) sections of the western North Pacific, respectively, based on all the BGC-Argo profiles (N=7120, see Fig. 2). The errorbar represents one standard deviation of the mean MLD in each month.

Reference:

Feucher, C., Maze, G., & Mercier, H., 2019. Subtropical mode water and permanent pycnocline properties in the world ocean. Journal of Geophysical Research: Oceans,

124(2), 1139-1154.

2) Oxygen and carbon inventories should be estimated in each region and depth after classifying the water masses as described above. Subduction patches shallower than the permanent pycnocline are not isolated for long time because they dissipate in the next year. On the other hand, subduction below the permanent thermocline, where carbon can be sequestered from the atmosphere for long time, is the important transport process. It will be difficult to clarify the entire spatial distribution of patches below the permanent pycnocline and to estimate the amount of material transported by subduction using Argo dataset. However, it may be meaningful to calculate the mean value of the patches separately by area and depth, and compare them.

Reply: Following your suggestion, here we calculated the mean values of the patches separately for subtropical (i.e., south of 35° N) and subpolar (i.e., north of 35° N)) regions of the western North Pacific, and for each region, we also calculate separately for above and below the depth of permanent pycnocline (PP). The depths of PP in the subtropical and subpolar regions were referred as 450 m and 300 m, respectively (see our reply to the first major comment above, Figs. R1 & R2). For each layer (above or below the depth of PP) in each region, we quantified the number of subduction patches identified, mean ΔAOU, mean ΔDO, mean thickness (i.e., vertical extension) of the subduction patches, and the mean DO inventory based on the two methods (i.e., integrated area (IA), and peak height (PH) method).

The statistics are summarized in Table R1. Specifically, in the subpolar region, 34 (10.1%) and 141 (42.1%) subduction patches were identified above and below the depth of PP (i.e., 300m), and for each layer, the mean ΔAOU are -32.9 and -25.8 μmol/kg, mean ΔDO are 42.5 and 32.5 μmol/kg, mean thickness of 127.5 and 126.6 m, and the DO inventory$_{IA}$ are 92.6 and 61.2 g O_2 /m^2; in the subtropical region, 56 (16.7) and 104 (31.0%) of the subduction patches were identified above and below the depth of PP (i.e., 450m), and for each layer, the mean ΔAOU are -27.2 and -28.5 μmol/kg, mean ΔDO are 31.2 and 36.4 μmol/kg, mean thickness of 128.7 and 128.1 m, and the DO inventory$_{IA}$ are 51.7 and 64.3 g O_2 /m^2. In general, it is found that, (1) the vertical extension (i.e., thickness) of the subduction patches identified in each layer and in each region did not vary much between 126.6 m and 128.7 m; (2) the mean ΔAOU, ΔDO, and DO inventory were stronger above the depth of PP than those below the depth of PP in the subpolar region, yet the opposite case shows for subtropical region, where the mean ΔAOU, ΔDO, and DO inventory were weaker above the depth of PP than those below the depth of P; (3) the mean ΔAOU, ΔDO, and DO inventory in the subtropical region below 450 m were also weaker than those in the subpolar region above 300 m, which further supports the potential pathway shown in Fig. 7 that the subduction occurred in the northern KE (i.e., > 35° N, subpolar section) and the subducted water traveled south and deeper along isopycnal surface as illustrated in Fig. 1.

Accordingly, these additional results and analyses were added in the revised manuscript.

Table R1. Statistics on the subduction patches in the subtropical and subpolar sections

of the western North Pacific, for both above and below the depth of permanent pycnocline (PP) in each section. The depths of PP in the subtropical and subpolar sections were referred as 450 m and 300 m, respectively, based on Figs. R1 & R2. Note that the percentages in the third column (i.e., Number of patches) refer to the ratios between the number of subduction patches identified in each category and the total number of subduction patches identified (N=335), and "H" refers to the thickness (i.e., vertical extension) of the subduction patch.

Region	Layer	Number of patches	Mean ΔAOU (μmol/kg)	Mean ΔDO (μmol/kg)	Mean H (m)	DO $inventory_{IA}$ (g O_2 /m^2)	DO $inventory_{PH}$ (g O_2 /m^2)
Subtropical	< 450 m	56 (16.7%)	-27.2±17.7	31.2±20.4	128.7±27.1	51.7±45.9	132.1±106.2
	≥ 450 m	104 (31.0%)	-28.5±15.3	36.4±18.0	128.1±25.8	64.3±50.6	161.5±103.0
Subpolar	< 300 m	34 (10.1%)	-32.9±15.5	42.5±17.7	127.5±35.0	92.6±59.7	197.5±115.3
	≥ 300 m	141 (42.1%)	-25.8±15.9	32.5±20.9	126.6±23.2	61.2±53.1	142.1±108.1
Whole area	< 450 m	161 (48.1%)	-29.7±16.7	36.7±19.7	126.8±26.8	68.5±52.8	160.5±108.0
	≥ 450 m	174 (51.9%)	-25.6±15.2	32.5±19.8	128.2±25.1	59.4±52.5	144.3±108.0

Specific comments

Line133-136: The material transport by subduction is a topic of great interest to Biogeochemical scientists. However, "spicity" is not a familiar parameter, so a detailed explanation of spicity is needed.

Reply: Sea water is a two-component system. Water mass anomaly is commonly analyzed in term of (potential) temperature and salinity anomaly. Isopycnal analysis is also widely used. By definition, temperature and salinity anomaly on an isopycnal surface is density compensated; thus, water mass anomaly on an isopycnal surface is commonly described in term of another thermodynamic variable, which is called spice, spiciness or spicity. Over the past decades, there have been different definitions of such a thermodynamic variable; however, a most desirable property of such a thermodynamic function is that it is orthogonal to the density. Recently, Huang et al. (2018) proposed a potential spicity function (π) by the least square method, which is practically orthogonal to the potential density, with the root-mean-square of angle deviation from orthogonality at the value of 0.0001°. Therefore, combining density and spicity gives rise to an orthogonal coordinate system, and it is the thermodynamic variable we used in this study. More description on spicity was added in the revision.

Reference:

Huang, R. X., L.-S. Yu and S.-Q. Zhou (2018). Potential spicity defined by the least square method. Journal of Geophysical Research-Oceans, 123, 7351-7365.

Line242-244: The authors assume that the lifetime of subduction patches is one year. However, it is expected to vary depending on the depth and the region. This calculation should be reconsidered.

Reply: A similar comment was also raised by Reviewer # 1 (Joan Llort). Converting carbon and oxygen inventories to export fluxes requires some knowledge of subduction rates, which can vary exponentially from the surface to the deep ocean. To be conservative, we assume the lifetime of subduction patches to be on an annual scale based on the seasonal statistics of the subduction we detected. Yet this would still involve some uncertainties, considering the dynamics of subduction at different depths and in different regions. However, we did not find any better way to resolve the subduction rates. As such, to avoid any misleading results and analyses, we removed the calculations of fluxes in the revision.

Fig.4b: The anomalies of spicity, indicated by boxes in Fig.4b, is unclear.

Reply: It could be caused by the reduced resolution in PDF file. The anomalies of spicity in Fig. 4b are clearly shown in our original figure at full resolution. We will make sure the original figure will be used when it is to be published.

Line297-303: The fact that anomalies were observed four consecutive profiles does not mean a sustained or a large spatial subduction event. A further analysis of the water mass using the surrounding water temperature and salinity would be necessary to show the spread of the subduction.

Reply: We did further analysis of the water mass. Fig. R2 shows the corresponding time series of temperature (a), salinity (b) and potential density (c). Corresponding to the anomalies identified in boxes 1-3 in Fig. 4b-4d, we found that salinity shows similar anomalous patches. As such, we suspect that the distinct and continuous water patches observed from the four consecutive profiles in box 3 were mostly likely resulted from one subduction event. We added this analysis in the revision.

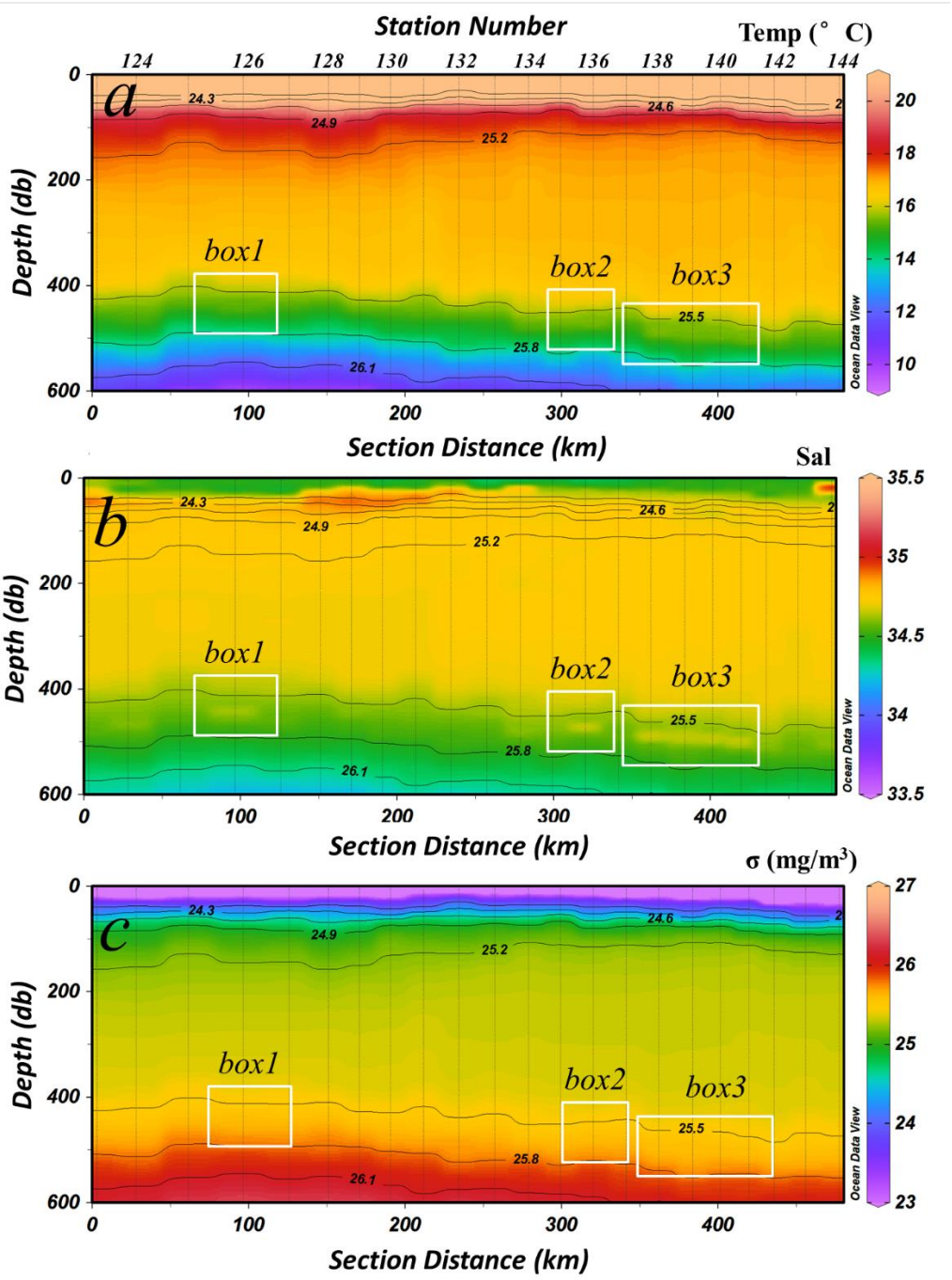

Fig. R2 Time series of temperature (a), salinity (b) and potential density (c) of float MR2901556 between July 28th, 2014 and August 18th, 2014.

Fig.5: The distributions of EKE and SLA are unclear. It might be better to use only contour line instead of color gradients.

Reply: Fig. 5 is updated in the revision. We added contour lines on the color map to better show the distributions of EKE and SLA.

Fig.6: I do not think it is necessary to apply smoothing to these graphs; it would be easier to show them in a monthly summary, as in Fig.2S.

Reply: Different from Fig. S2, we want to resolve the temporal distribution of each term (i.e., the number of patches, integrated AOU anomaly, integrated spicity anomaly, and integrated DO anomaly) on a finer time scale (i.e., daily) in Fig. 6. The main reason for a 7-point smoothing was to reduce the noise. For example, Fig. R3 shows the data plots with and without smoothing. Clearly, the time series are somewhat noisier without smoothing, making it more difficult to interpret. However, with a 7-point smoothing, the temporal variation patterns were much clearer in each quantity, with most signals being observed between March (the maximum) and August.

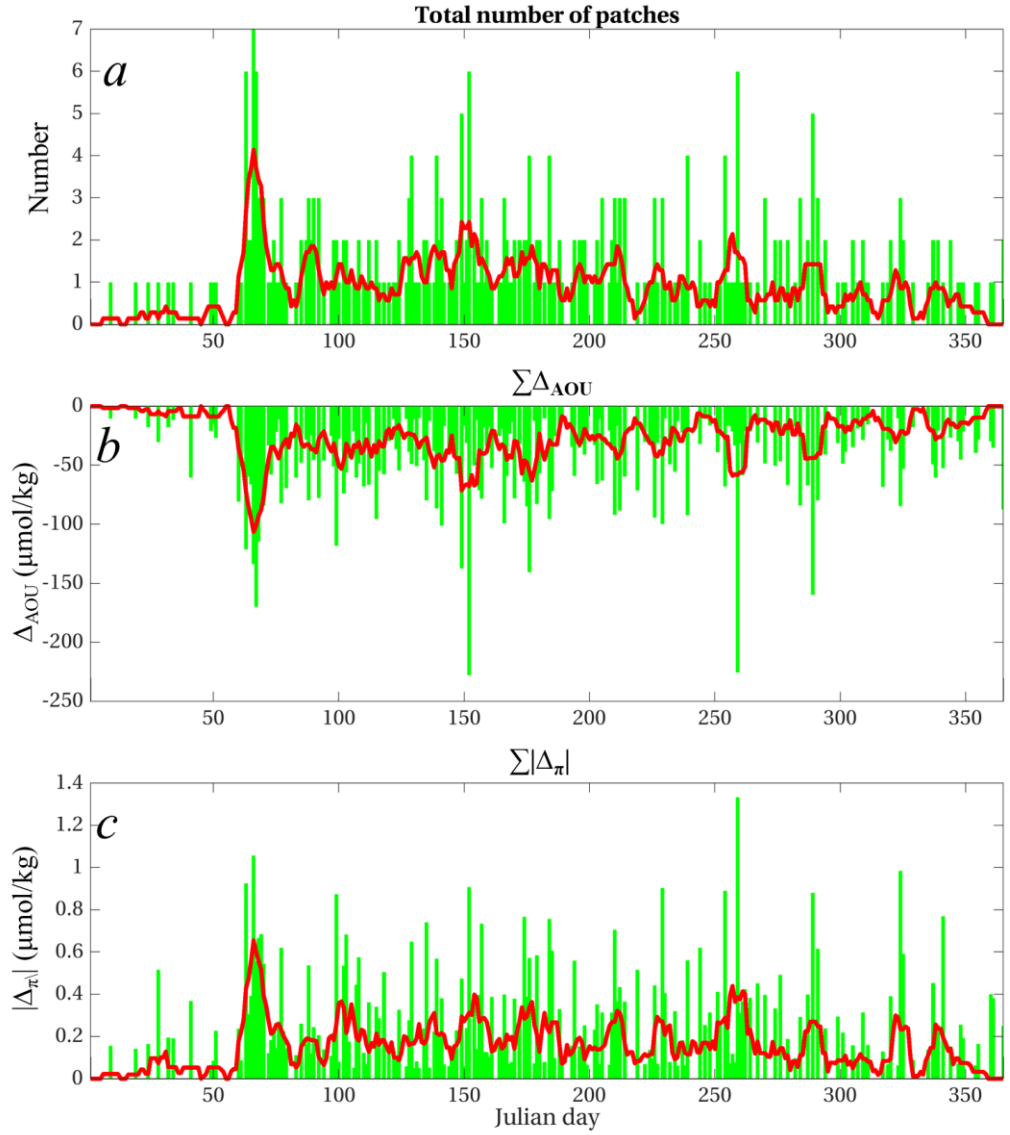

Fig. R3 Temporal distribution of the number of patches (a), integrated AOU anomaly (b), and integrated π anomaly (c), by Julian day. Note that the green bars are the quantities on each day without smoothing, and the red curves are based on 7-point smoothing.

Line 398: AOU or ΔAOU?

Reply: Corrected. It is ΔAOU.

Line 403-404: The authors mention high levels of phytoplankton production as the cause of

the strong AOU anomaly from March to August, but it should be clear whether this indicates the release of oxygen from phytoplankton production or the consumption of oxygen by decomposing large amount of organic matter.

Reply: Clarified in the revision, the strong AOU anomaly indicates the release of oxygen from phytoplankton production.

Table2: I cannot understand what inventories and exports on the peak height mean.

Reply: More description on the peak height calculations was added in the revision. Take the oxygen inventory as an example, we firstly integrated the DO anomaly against the referred baseline (Eq. R1), this integrated anomaly represents the inventory of anomalous DO resulted from the subduction patch, this quantity was illustrated as the area with dash lines crossed on the left panel in Fig. R4. We also quantified the DO inventory using peak height method (Eq. R2). Here Δ_{DO_peak} is DO anomaly referred to the baseline at the peak and H is the vertical scale of the subduction patch [see Section 2.2.1 for how a peak was detected and how H was defined]. The shaded area on the right panel in Fig. R4 represents the derived DO inventory using Eq. R2. This derived quantity represents the maximum potential of DO inventory within the subduction patch.

$$\text{Oxygen Inventory}_{IA}\ (\text{g O}_2/\text{m}^2) = \sum_{z=p1}^{z=p2} \Delta DO_Z \qquad \text{(Eq. R1)}$$

$$\text{Oxygen Inventory}_{\_PH}\ (\text{g O}_2/\text{m}^2) = \Delta_{DO\_peak} \times H \qquad \text{(Eq. R2)}$$

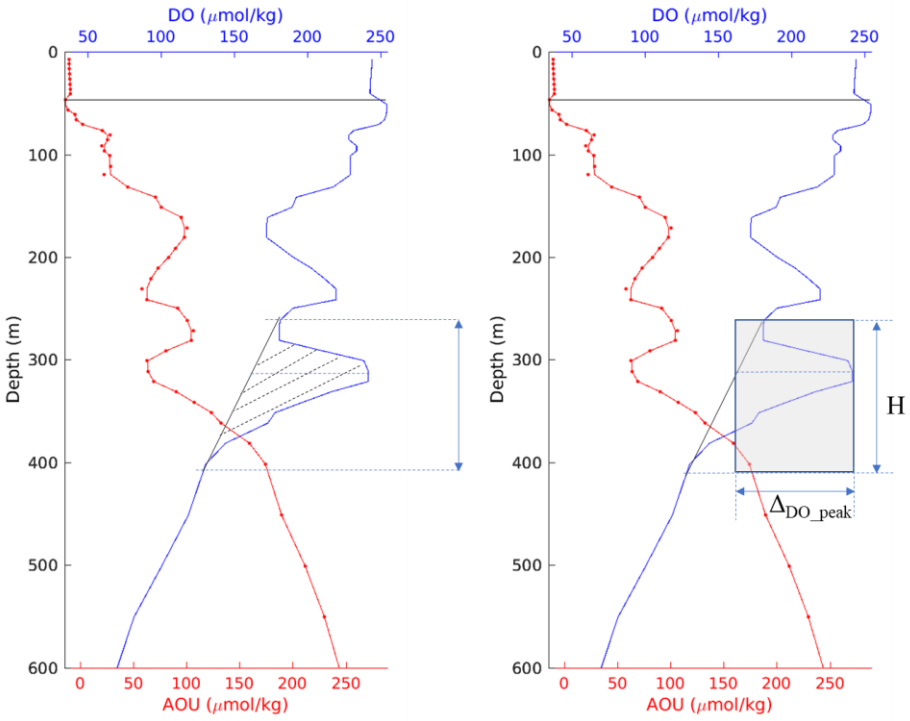

Fig. R4 Illustration of DO inventory calculated from Eq. R1 (left panel) and Eq. R2 (right panel). The DO inventory using peak height method (Eq. R2) represents the maximum potential of the DO inventory from the subduction patch.

It should be noted that, following suggestions from Reviewer #1 comments, we removed the calculations of fluxes in the revision.

Line 463-469: The oxygen export rate calculated here should not be compared to the oxygen consumption rate in the Southern Ocean.

Reply: Considering the difficulty in parameterizing subduction rates and the large potential uncertainties involved, we removed the fluxes-related results and analyses in the revision. Please see our related replies to the comments from Reviewer # 1 for details.